

Low Cost Assessment Of Connector Performance

**Alyse R.
Coates**

**Alexandros
Gavrilakis**
De Montfort University, Leicester, UK

**Muhammed
Al-Asadi**

**Alistair P.
Duffy**

**Kenneth G
Hodge**

**Arthur J
Willis**

Brand-Rex Ltd, Glenrothes,
Scotland

alyse@dmu.ac.uk alex@dmu.ac.uk

apd@dmu.ac.uk

khodge@brand-
rex.com

awillis@brand-
rex.com

Abstract

From an electromagnetic interference perspective, it is widely acknowledged that connectors are the most sensitive components in cascaded copper systems. Twisted pair connectors are inherently poorly suited to radiation rejection through their design. It is useful, therefore, to be able to quantify the radiation performance for connectors to enable quantitative assessments of interference rejection or to provide input to numerical models used to predict interference performance of cascaded systems. This latter point is particularly important, as direct incorporation of connectors into numerical models using a reasonable computational resource in a reasonable time is generally extremely difficult due to the complexity of the connectors. In this paper the electromagnetic emissions from a plug-in-socket combination and from a cable with no connector are measured using a 'Stripline Cell' and the dipole moments for each device and each twisted pair are presented.

1. Introduction

In order to create a better connector, many different designs could be produced, prototyped and tested, however this is expensive, time consuming and unpredictable. Another technique is to simulate the different designs, but this requires a lot of processing power and modelling the fine details can make the simulations overly complicated. These approaches are particularly inefficient if the performance of an installed system is required, taking into account the general EMC performance of local structures. It is perhaps sensible therefore to use a combination of testing and modelling to simplify the modelling by eliminating the need for simulating some of the fine detail. For example, if the emissions from a standard plug and connector combination are known in terms of E_x , E_y , E_z , H_x , H_y and H_z then it can simply be inserted into the simulation as a 'black box' that reacts to certain stimuli in a predefined manner. Simplifying the modelling in this manner should provide the ability to simulate scenarios more rapidly and hence lead to faster prototyping.

In such measurement techniques as the mode stirred chamber method (see 'Determining Cable Shield Behaviour') only the total power emitted from the device under test can be measured. However, this is not sufficient, when the electromagnetic emissions from the device need to be broken down into the three orthogonal directions. The most convenient method of doing this is to calculate the 'dipole moments' of the device. The dipole moments can best be viewed as a method of decomposing the emissions from a device into six radiating components, three orthogonal electric field radiators (E_x , E_y , E_z) and three orthogonal magnetic field radiators (H_x , H_y , H_z). All of these are functions of frequency and can be determined by taking measurements of the radiating device in a manner that allows both the directivity and magnitude of the fields to be taken into account.

2. Obtaining the Dipole Measurements for the Device Under Test

Measurements for the dipole moments were taken using a parallel plate 'Stripline Cell' (which is shown diagrammatically in Figure 1). The stripline is a lower cost alternative to the TEM (or Crawford) Cell, which uses three parallel plates and has enclosed sides to improve the accuracy of the field definition within the measurement environment. The stripline cell consists of two metallic plates, which are parallel in the middle section, which forms a cube of 0.8m, but taper together at their ends, forming two output ports. The tapers are designed to maintain constant impedance along the length of the cell. This apparatus is placed above a ground plane at a distance equal to its height. The device under test is then placed in the centre of the cell and connected to the output port of a network analyser. To ensure adequate field uniformity, the test object was limited to a cube of no more than 200mm on each side. The output ports of the cell are then connected via a junction to the input port of the network analyser. The open sides of the stripline are not a significant issue, providing the cell is sufficiently distant from other structures to avoid interference with the fringing fields. The parallel plates permit transverse electromagnetic (TEM) propagation with a reasonably well-defined and well-conditioned electric field. Hence, for a device under test, the radiated power (in the direction between the plates) can be measured at the tapered ends of the stripline using a combiner (or splitter) and a network analyser.

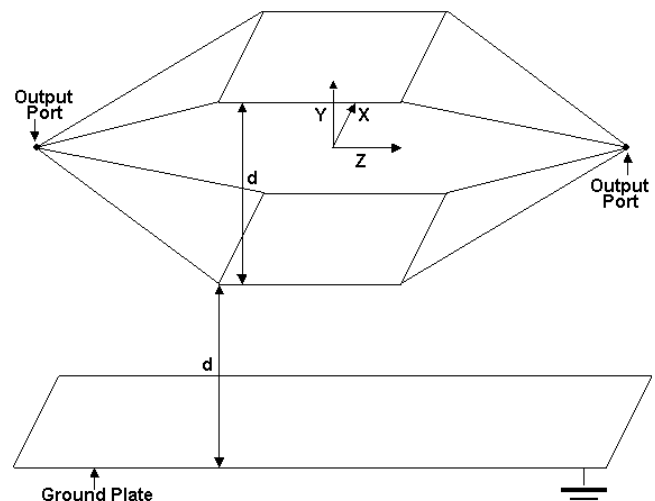


Figure 1. A schematic of the stripline cell.

When an arbitrary current source (the device under test) is introduced inside the waveguide it will generate electric and magnetic fields in both the forward direction (E^+ , H^+) and the backward direction (E^- , H^-). The simplest way to calculate these

fields [1] is when both the current source and the power at each output port are known. The total field is the sum of an expansion coefficient a_n or b_n (which are functions of the current source value) and the field at each transverse electromagnetic mode (n).

$$\overline{E}^{(+)} = \sum a_n \overline{E}_n^{(+)} \quad (1)$$

$$\overline{E}^{(-)} = \sum b_n \overline{E}_n^{(-)} \quad (2)$$

$$\overline{H}^{(+)} = \sum a_n \overline{H}_n^{(+)} \quad (3)$$

$$\overline{H}^{(-)} = \sum b_n \overline{H}_n^{(-)} \quad (4)$$

If a parallel plate waveguide is used, where the guide has no sides and the source is placed at the centre of the cell only the dominant TEM mode (n=0) is present therefore only the a_0 and b_0 coefficients need to be determined for Equations 1-4.

However, in virtually all circumstances the detail of the current source is unknown so the concept of dipole moments has to be introduced into the determination of the values of the a_0 and b_0 coefficients. The coefficients a_0 and b_0 are related to the electric (m_e) and magnetic (m_m) dipole moments using Equation 5 and 6.

$$a_0 = -\frac{1}{2}(\overline{m}_e + jk\overline{M}) \cdot \overline{e}_0 \quad (5)$$

$$b_0 = -\frac{1}{2}(\overline{m}_e - jk\overline{M}) \cdot \overline{e}_0 \quad (6)$$

Where \overline{e}_0 , q and \overline{M} are defined in Equations 7, 8 and 9 respectively.

$$\overline{e}_0 = q\overline{y} \quad (7)$$

$$q = \frac{\sqrt{Z_0 \cdot P}}{b} \quad (8)$$

$$\overline{M} = \overline{m}_m X \overline{z} \quad (9)$$

Where \overline{z} is the unit vector along the longitudinal axis of the cell, \overline{e}_0 is the normalized transverse vector electric field inside the cell, \overline{y} is the unit vector perpendicular to the parallel plates, Z_0 is the impedance of the cell (150Ω), P is the power supplied to the cell, b is the separation distance between plates in metres (0.8m) and k is the free space wave number as defined in Equation 10.

$$k = \frac{2 \cdot \pi \cdot f}{c} \quad (10)$$

Where f is the frequency and c is the speed of electromagnetic propagation in free space (2.99792x10⁸ m/s).

Hence the dipole moments (m_e and m_m) can be used to quantify precisely the emissions from a dipole. But if it is assumed that any device can be represented by three orthogonally directed dipoles, then the emissions can be broken down into their constituent parts (E_x , E_y , E_z , H_x , H_y and H_z) using the dipole moments and reconstructed from the magnitudes (m) and phases (Ψ) using Equations 11 to 16.

$$E_x = m_{ex} \angle \Psi_{ex} \quad (11)$$

$$E_y = m_{ey} \angle \Psi_{ey} \quad (12)$$

$$E_z = m_{ez} \angle \Psi_{ez} \quad (13)$$

$$H_x = m_{mx} \angle \Psi_{mx} \quad (14)$$

$$H_y = m_{my} \angle \Psi_{my} \quad (15)$$

$$H_z = m_{mz} \angle \Psi_{mz} \quad (16)$$

The ubiquitous nature of four pair UTP cable is the reason that this was used throughout this paper, the method works equally well with other connector systems or small devices. The main limitation on the method is that the device under test should not be more than 1/3 of the height of the cell.

The devices under test in this paper were firstly a length of UTP cable with a plug and socket as the device under test. Then, for comparison purposes, just a length of UTP cable was tested. For each 'device' one end was connected to the output of the network analyser via a balun whilst the other end was connected to a matching load via a second balun. Each coloured pair of twisted wires (see Figure 2) was measured separately so the overall contribution to the emissions from each pair could be determined.

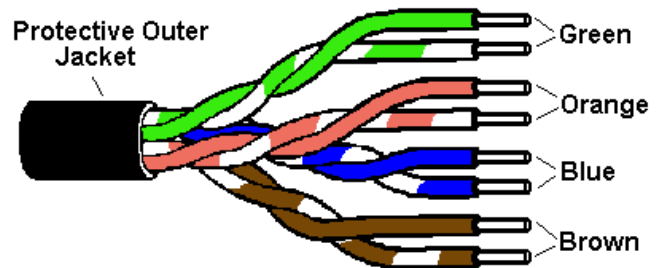


Figure 2. Diagram of twisted pair cable.

In order to measure the dipole moments, the devices under test had to be positioned in six different orientations as specified in Figure 3. Both the axes of the cell (X, Y and Z) and of the device under test (x, y and z) remain constant relative to what they describe (cell or device under test) throughout, though they are rotated relative to each other. The devices under test were placed between the parallel plates using a low dielectric constant mount.

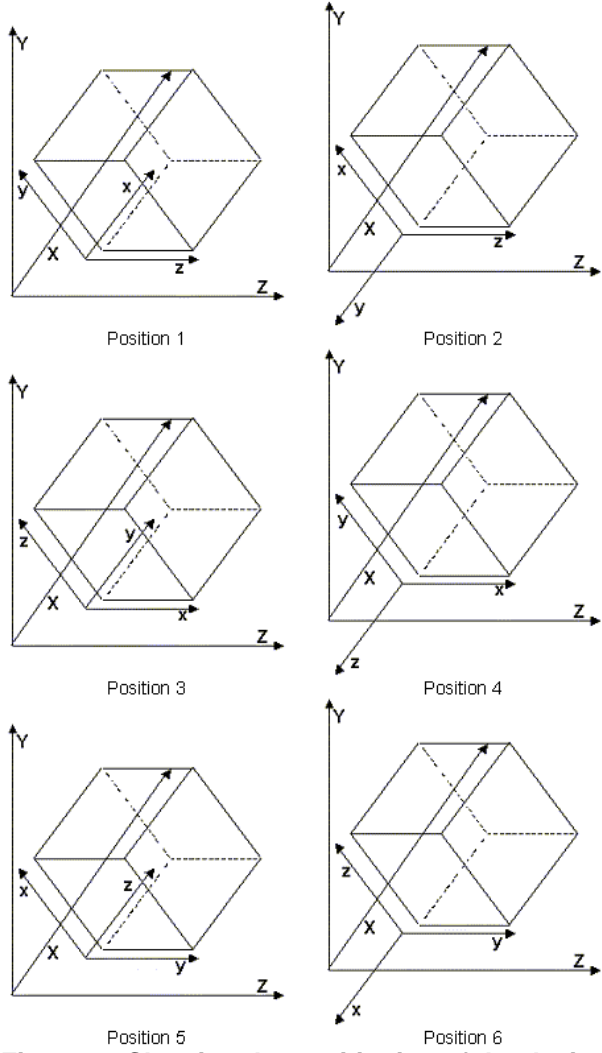


Figure 3. Showing the positioning of the device under test in the cell.

In order to separate the contributions of the electric and magnetic dipole moments simple addition (electric dipole moments) and subtraction (magnetic dipole moments) of the coefficients a_0 and b_0 is required. This addition and subtraction is carried out whilst the measurements are being taken by inserting either a 0° hybrid junction (see Figure 4) or a 180° hybrid junction (see Figure 5) in between the outputs of the cell and the input of the network analyser.

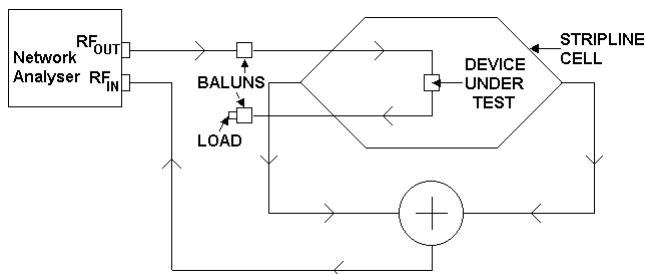


Figure 4. Schematic of the circuit to measure the sum of the outputs (P_s).

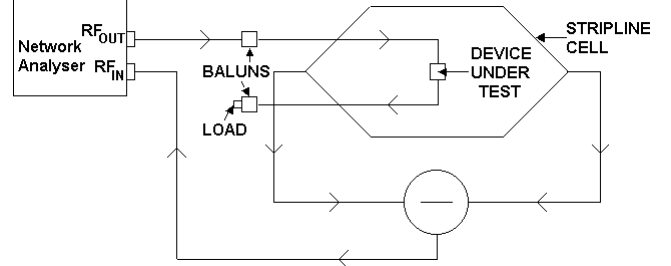


Figure 5. Schematic of the circuit to measure the difference of the outputs (P_d).

The powers detected at the output of the junction which relate to the sum of coefficients (P_{si}) and their difference (P_{di}) are given by Equations 17 and 18, where the 'i' stands for the power at the i^{th} device under test orientation (1 to 6, see Figure 3).

$$P_{si} = |a_0 + b_0|^2 = |\overline{m_e} \cdot \overline{e_0}|^2 \quad (17)$$

$$P_{di} = |a_0 - b_0|^2 = k^2 |\overline{M} \cdot \overline{e_0}|^2 \quad (18)$$

In order to obtain the electric and magnetic dipole moment amplitudes (m_e and m_m) from the power responses at the 6 different orientations Equations 19 to 24 are used. The relative phases between the moments can also be found [1], however these are not used herein.

$$m_{ex}^2 = \frac{(P_{S1} + P_{S2} - P_{S3} - P_{S4} + P_{S5} + P_{S6})}{2 \cdot q^2} \quad (19)$$

$$m_{ey}^2 = \frac{(P_{S1} + P_{S2} + P_{S3} + P_{S4} - P_{S5} - P_{S6})}{2 \cdot q^2} \quad (20)$$

$$m_{ez}^2 = \frac{(-P_{S1} - P_{S2} + P_{S3} + P_{S4} + P_{S5} + P_{S6})}{2 \cdot q^2} \quad (21)$$

$$m_{mx}^2 = \frac{(P_{d1} + P_{d2} - P_{d3} - P_{d4} + P_{d5} + P_{d6})}{2 \cdot k^2 \cdot q^2} \quad (22)$$

$$m_{my}^2 = \frac{(P_{d1} + P_{d2} + P_{d3} + P_{d4} - P_{d5} - P_{d6})}{2 \cdot k^2 \cdot q^2} \quad (23)$$

$$m_{mz}^2 = \frac{(-P_{d1} - P_{d2} + P_{d3} + P_{d4} + P_{d5} + P_{d6})}{2 \cdot k^2 \cdot q^2} \quad (24)$$

Finally the amplitude of the total power emitted by the devices (P_t) can then be obtained from the moment amplitude results using Equation 25.

$$P_t = \frac{40 \cdot \pi^2}{\lambda^2} \left[m_{ex}^2 + m_{ey}^2 + m_{ez}^2 + k^2 (m_{mx}^2 + m_{my}^2 + m_{mz}^2) \right] \quad (25)$$

3. Results

Each of the devices under test (the cable and the connector) were tested using the method described in this paper. For each device, each pair of twisted wires were connected up and measured separately, so any differences between the responses could be examined. Also the contribution of each pair to the total emitted power could be observed.

Figures 6 and 7 show the differences and similarities between the sums of the emitted powers received at the outputs of the stripline cell (P_s), for firstly the cable and then the connector when the device under test is placed in the six positions indicated in Figure 3. It can be clearly seen that the emissions from a specified pair (in this case the brown pair) have many similar features in all six positions. It can also be seen that the emissions from the connector are greater than those from just the cable.

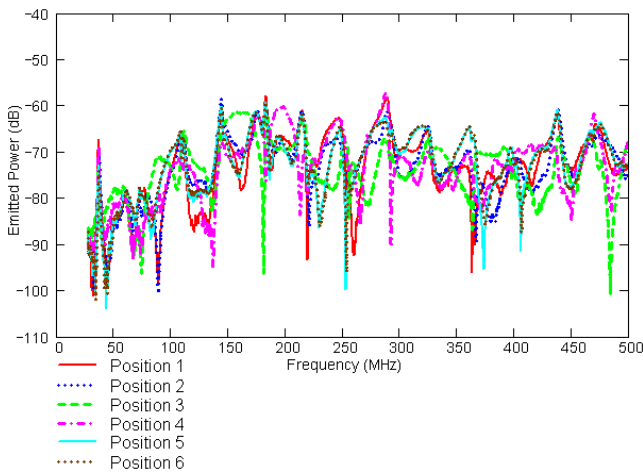


Figure 6. The emissions from the brown pair in the cable measured using the addition junction.

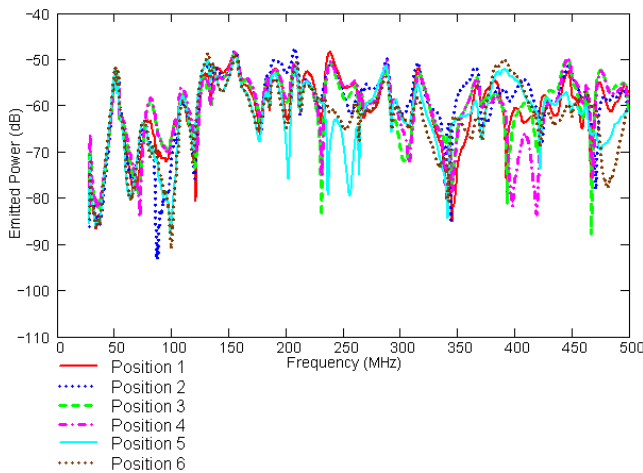


Figure 7. The emissions from the brown pair in the connector measured using the addition junction.

In Figures 8 and 9 the difference of the emitted powers (P_d) measured at the outputs of the stripline cell are shown for all the twisted pairs whilst the devices under test remain stationary in position 5. It can be seen that whilst each of the responses have similar sharp features to those observed in Figures 6 and 7, the responses for the different wire pairs vary greatly from each other.

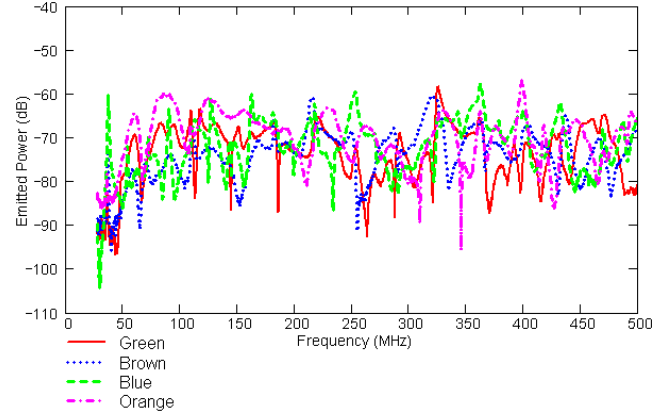


Figure 8. The emissions measured in position 5 for the cable, using the subtraction junction.

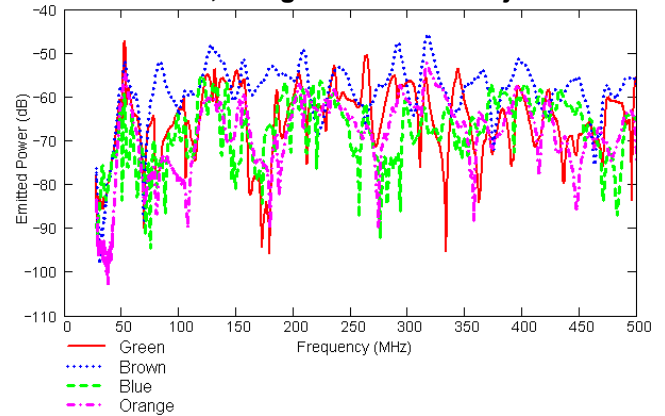


Figure 9. The emissions measured in position 5 for the connector, using the subtraction junction.

It can be seen from Figures 6 to 9 that all of the emission responses contain strong features (sudden peaks or troughs) and the amplitude of the responses vary greatly with frequency. It can also be seen that whilst the emission responses remain reasonably consistent for a specific pair whilst the device position is altered, the responses for the different twisted pairs vary widely from each other. It has also been noted that the responses obtained for the two devices under test are very different from each other in terms of both amplitude and the positioning of the features, in order to closer examine these differences the emissions from the same pair of wires in the same position for each device were compared.

When the emissions from an identical pair of wires passing through the connector and through just the cable are compared it is immediately evident that the emissions from the connector exceed those from just the cable on its own, as would be expected. However, the magnitude of the difference can clearly be seen in Figures 10 to 13.

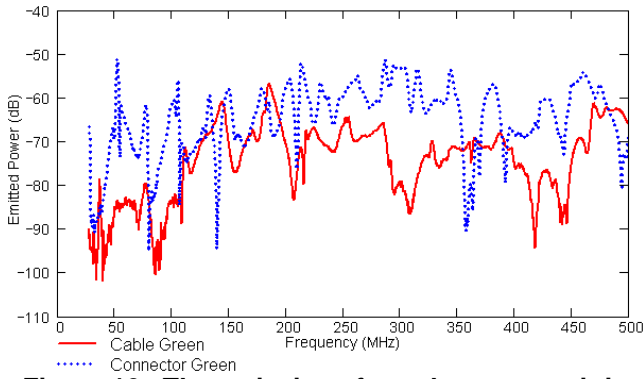


Figure 10. The emissions from the green pair in position 3 measured using the addition junction.

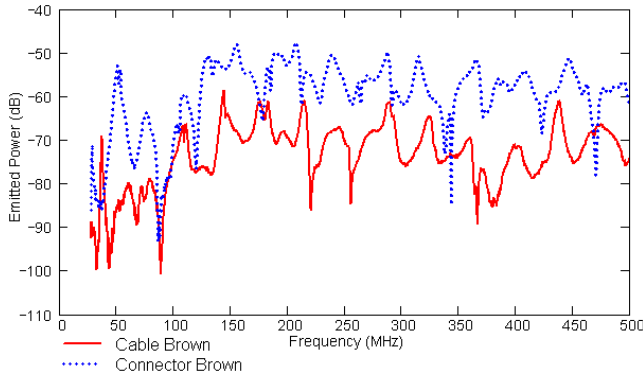


Figure 11. The emissions from the brown pair in position 3 measured using the addition junction.

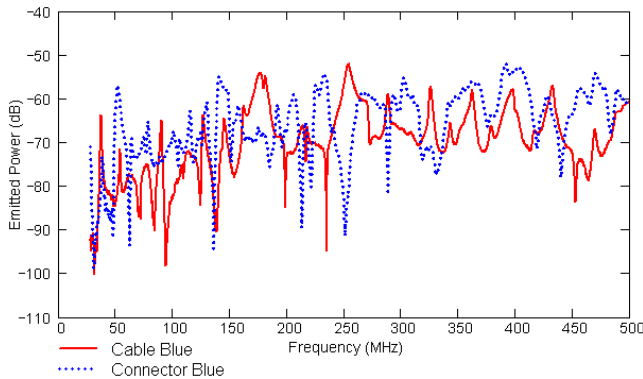


Figure 12. The emissions from the blue pair in position 4 measured using the subtraction junction.

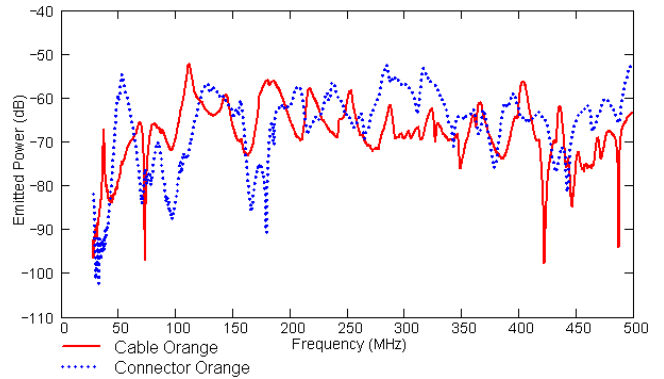


Figure 13. The emissions from the orange pair in position 4 measured using the subtraction junction.

When the electric dipole moments were calculated from the emissions responses using Equations 19 to 21, the differences between the cable and connector results were immediately evident (see Figures 14 to 17).

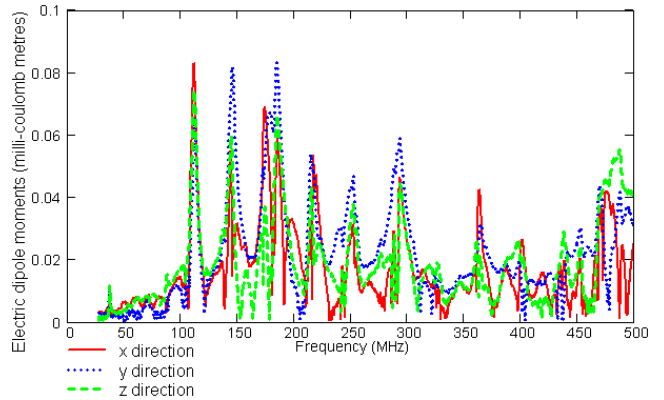


Figure 14. Electric dipole moments from the green pair in the cable.

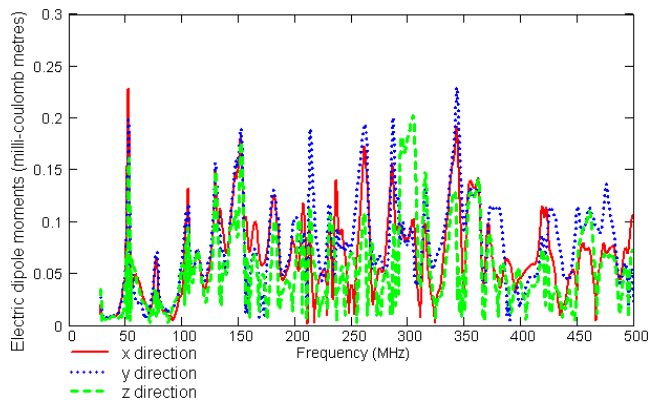


Figure 15. Electric dipole moments from the green pair in the connector.

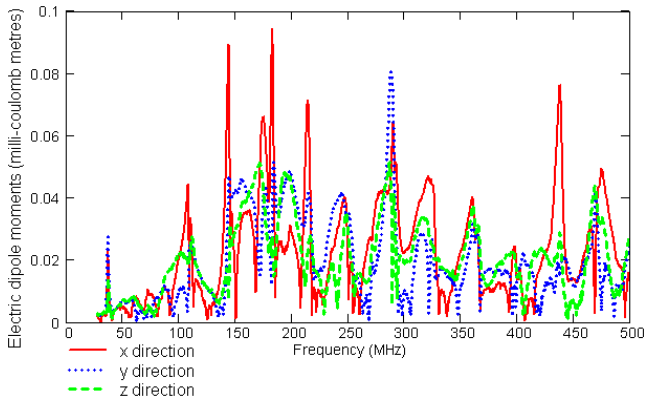


Figure 16. Electric dipole moments from the brown pair in the cable.

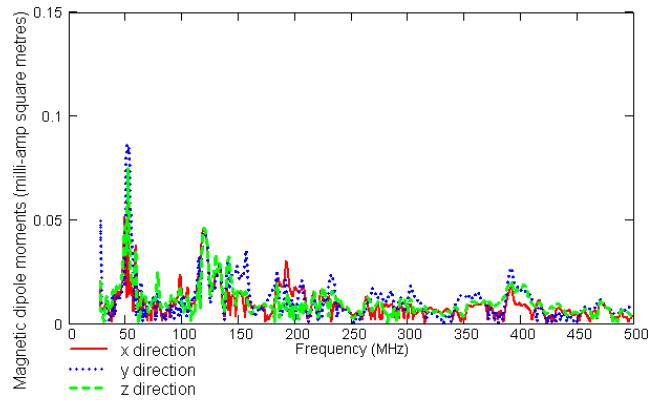


Figure 19. Magnetic dipole moments from the blue pair in the connector.

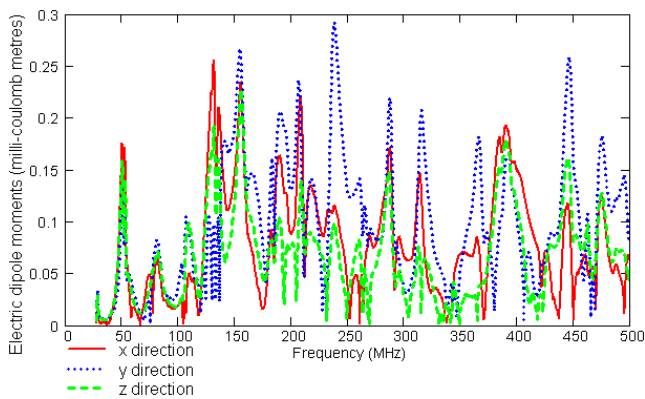


Figure 17. Electric dipole moments from the brown pair in the connector.

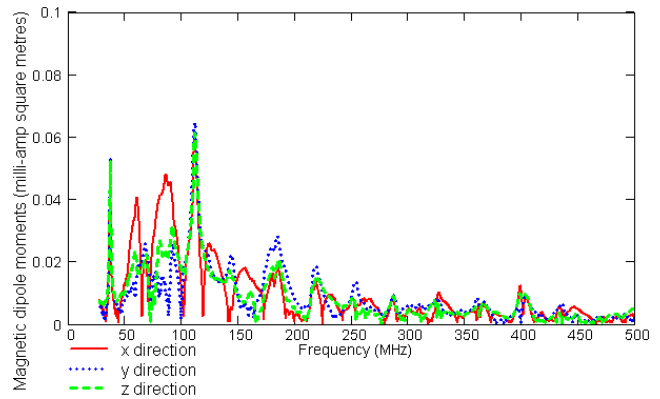


Figure 20. Magnetic dipole moments from the orange pair in the cable.

The magnetic dipole moment amplitudes were obtained from the emissions responses using Equations 22 to 24, as can be seen in Figures 18 to 21. As with the electric dipole moments, the amplitude of the responses varied greatly between the two devices.

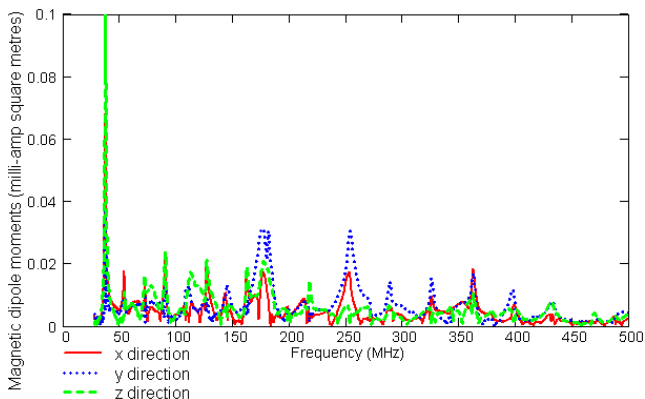


Figure 18. Magnetic dipole moments from the blue pair in the cable.

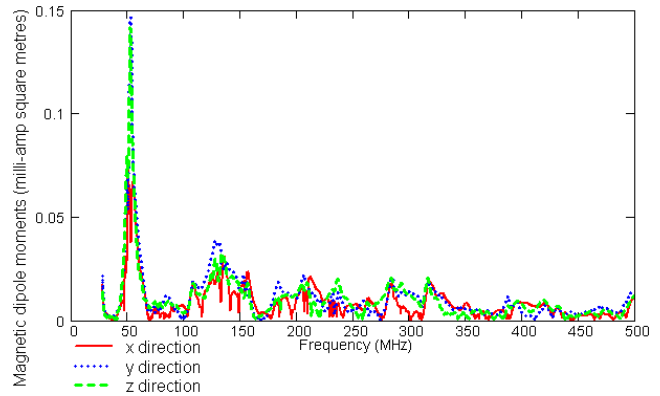


Figure 21. Magnetic dipole moments from the orange pair in the connector.

Both sets of dipole moment responses show strong features that are consistent between the three orthogonal dipoles that represent a specific device and twisted pair. However, the dipole moment responses vary greatly between the different pairs, suggesting that the total emitted power contributed by each pair is also different. This hypothesis was tested by using the dipole moment responses to calculate the total power emitted by each pair in each device using Equation 25.

It can be seen from Figure 22 that the total power emitted by each pair in the cable is rather similar, though the emitted power does vary with both pairs and frequency. However, the total power emitted by the connector is strongly dependant on the twisted pair being tested, see Figure 23. It can be seen by comparing Figures 22 and 23 that more power is emitted from the connector than from just the cable, to quantify this difference the total power emitted by each pair in each device was averaged over the entire frequency range, these results are shown in Table 1.

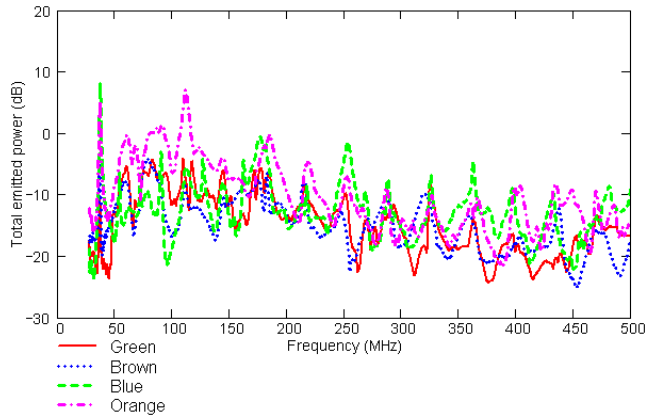


Figure 22. Total power emitted from the cable.

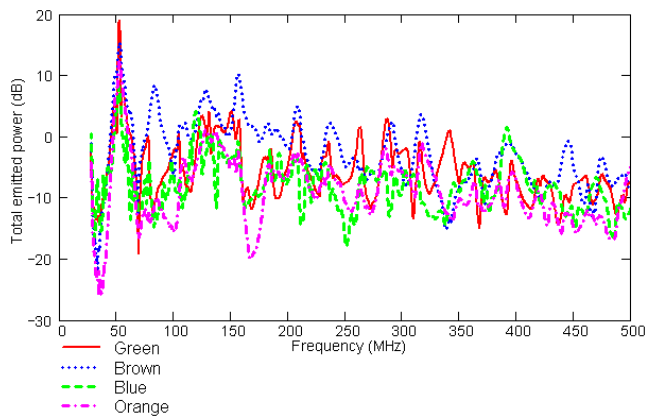


Figure 23. Total power emitted from the connector.

It can be seen from Table 1 that the average power emitted by a pair in the connector is up to 13dB greater than that which is emitted by the same pair in just the cable on its own. It can also be seen that the amount of power emitted by each cable pair is different, probably due to the positioning of the pair within the cable.

Table 1. Showing the average ‘total emitted power’ (in decibels) for each device and pair.

	Green	Brown	Blue	Orange
Cable	-14.8	-15.1	-12.8	-10.4
Connector	-5.6	-2.8	-7.9	-9.0

4. Conclusion

The method described in this paper can be used to obtain the dipole moments of any device (provided certain criteria, such as device size, are met), quickly, easily and relatively inexpensively. These dipole moments can, in turn, be used to predict the total emitted power and (if phase is taken into consideration) the radiation patterns from the device.

The dipole moments obtained for both a cable and a connector were used in this manner to obtain the total emitted power as a function of frequency. These results show how much extra power is radiated from a connector relative to a cable and hence demonstrate the need to fully characterise and examine these emissions.

In this paper a method has been demonstrated by which a complex electromagnetic device can be broken down into six dipoles that can be used to represent its behaviour. These representative dipoles can then be used in, for example, numerical modelling to predict the emissions from systems of which this device is only a part.

5. References

[1] Koepke, G. H., Ma, M. T., and Bensema, W. D. *NIST Technical Note 1326: Theory and Measurements of Radiated Emissions Using a TEM Cell*, United States: National Institute of Standards and Technology, 1989.

Author Biographies

Biographies for Alyse R. Coates and Alexandros Gavrilakis can be found in the paper “Determining Cable Shield Behaviour” in Session 16.

The biography for Muhammed Al-Asadi can be found in the paper “Input Impedance of Irregular Cascaded Systems” in Session 11.

The biographies for Alistair P. Duffy, Kenneth G Hodge and Arthur J Willis can be found in the paper “Technology Forecasting Techniques in Communications” in Management Session 1.